BNL-107475-2015-JA

(*J. Chem. Phys.* **142**, 044106 (2015)

Multi-layer Lanczos iteration approach to calculations of vibrational energies and dipole transition intensities for polyatomic molecules

Hua-Gen Yu[1]

Department of Chemistry, Brookhaven National Laboratory, Upton, NY 11973-5000, USA

(January 29, 2015)

Abstract

We report a rigorous full dimensional quantum dynamics algorithm, the multi-layer Lanczos method, for computing vibrational energies and dipole transition intensities of polyatomic molecules without any dynamics approximation. The multi-layer Lanczos method is developed by using a few advanced techniques including the guided spectral transform Lanczos method, multi-layer Lanczos iteration approach, recursive residue generation method, and dipole-wavefunction contraction. The quantum molecular Hamiltonian at the total angular momentum $J = 0$ is represented in a set of orthogonal polyspherical coordinates so that the large amplitude motions of vibrations are naturally described. In particular, the algorithm is general and problem-independent. An application is illustrated by calculating the infrared vibrational dipole transition spectrum of CH_4 based on the *ab initio* T8 potential energy surface of Schwenke and Partridge and the low-order truncated *ab initio* dipole moment surfaces of Yurchenko and co-workers. A comparison with experiments is made. The algorithm is also applicable for Raman polarizability active spectra.

[1]E-mail:hgy@bnl.gov

1 Introduction

During the past decades, remarkable progress has been made in computational studies of rovibrational spectra of molecules.[1–10] Now rigorous full dimensional quantum dynamics calculations can be done for polyatomic molecules up to nine atoms.[11–16] Those great accomplishments become possible mainly due to the advent of efficient eigensolvers,[8,16–20] discrete variable representation (DVR) techniques,[21–29] multilayer basis set constructions,[10,15,16,28,30] and compact quantum Hamiltonian in optimally selected coordinates[1,6,7,11,12,14,15,31–33] in addition to the massive parallel computing of supercomputers. For high dimensional systems, their eigenvalues are often solved using an iterative diagonalization approach[8,19,34–41] based on a sparse Hamiltonian matrix. Among them the Lanczos algorithm[42] is one of the most used iterative methods. It needs only two Lanczos vectors to calculate eigenvalues which minimizes the core memory requirement.

The standard Lanczos algorithm is a powerful method to compute extreme and widely spaced eigenstates. In order to efficiently compute interior states in dense spectrum regions, where eigenvalues are clustered with small spacings, variants of spectral transform techniques[12,43–54] and projection or filter diagonalization methods[48,55–67] have been developed. Indeed, the spectral transform Lanczos method pioneered by Ericsson and Ruhe[43] has fully taken the advantage of the Lanczos method because the transformed spectrum of original dense one becomes a strongly dilated spectrum. Recently, Yu and Nyman[49,68,69] have developed an universal guided spectrum transform Lanczos (GSTL) method to avoid the difficulty occurring in the action of analytical spectral transform functions on Lanczos vectors.[43–46,50,51,54] In the guided spectral transform technique, the spectral transform functions are expanded a short series of classical or formally orthogonal polynomials of Hamiltonian. As a result, the spectral transform function-vector products can be performed as the normal Hamiltonian-vector products in the Lanczos recurrence. The GSTL approach has been widely used in quantum reactive scattering (e.g. see Refs.[8,70] and ref-

erences therein) and molecular spectroscopy[7,8,12] calculations including resonance states.[69] By using a divide and conquer strategy, we have developed a two-layer Lanczos algorithm[40,71] that is capable of solving the eigenvalue problem of polyatomic systems up to six atoms without any dynamics approximation.[12] It also makes possible the routine calculation of vibrational energies of four- and five-atom molecules,[6,7] once a global potential energy surface of molecule is provided. In addition, Wang and Carrington[13] have also developed a contracted Lanczos method that is capable of rigorously computing the eigenvalues of six-atomic systems.[13] The contracted Lanczos method is similar to the two-layer Lanczos algorithm but also contracting the basis functions in radial coordiantes.

The Lanczos algorithm has also been used to study the transition amplitudes[34] except for eigenvalues. Currently, the most powerful algorithm is the recursive residue generation method (RRGM) of Wyatt and co-workers[72–74] and its improved variants.[36,44,75–78] Those methods utilize the standard Lanczos recursion so that they are low storage methods. Nevertheless, it is well known, the Lanczos vectors are not orthogonal after a few tens of iterations due to the precision of machine. The loss of orthogonality will produce spurious states including the duplications of true eigenstates. Results[72,73] showed that the RRGM algorithm can calculate transition amplitudes accurately in spite of the loss of orthogonality of Lanczos vectors, and describe the degeneracy of energy levels correctly.[74,75] In the Lanczos eigenvector version of Chen and Guo[77,78] and the quasi-minimum residue (QMR) version of Yu and Smith,[76] the orthogonality issue is fixed by taking the Lanczos vector overlaps with the initial vector in calculations. An arithmetic average method[73,77–79] has been proposed to deal with the duplication problem for non-degenerate cases. The outcomes are very accurate. In particular, the improved RRGM version of Chen and Guo[77,78] is capable of computing all transitional amplitudes with a single Lanczos recursion.

However, compared to the energy level calculations, the exact full dimension studies of dipole transition intensities are still limited for large polyatomic molecules. It is ham-

pered by the requirement of at least one eigenstate wavefunction that is often expensive to be obtained for a high dimension problem. Since those Lanczos-based methods[44,76–79] are performed in original full dimension, they are applicable for polyatomic molecules with up to four atoms if no dynamics approximation is adapted. In order to overcome this difficulty, one common approach is to construct a compact basis set while not complicating the eigenvalue problem. For instance, the multiconfiguration time-dependent Hartree (MCTDH) methods use pruned bases.[10,28] Recently, Leclerc and Carrington[30] proposed a sum of product basis method to calculating vibrational spectra without storing full-dimensional vectors.

In this work, we develop an efficient algorithm for studying large molecules, based on the Lanczos recursion, the spectral transform technique, the RRGM approach, and the basis set contraction. Theory is presented in Sec. 2 whereas an application to CH_4 is described in Sec. 3. Finally, a short conclusion is in Sec. 4.

2 Theory

In this section, we describe the multi-layer Lanczos iteration algorithm to calculate vibrational energies, wavefunctions and dipole transition intensities of polyatomic molecules. Basically, the algorithm is an extension of our two-layer Lanczos method[40,71] by implementing with the recursive residue generation method (RRGM),[44,72–75] the Green function-guided spectral transform technique in formally orthogonal Lanczos polynomials,[12,69] and DVR contraction and pre-screening enhancement.

2.1 Hamiltonian and guided spectral transform Lanczos method

Following previous studies[6,7,31,32,80–84] the molecular vibrational Hamiltonian is expressed in a set of orthogonal polyspherical coordinates. For a system with N atoms, the $(3N-6)$ internal variables are defined by $(N-1)$ radial coordinates ($\mathbf{R} = \{r_1, r_2, \cdots, r_{N-1}\}$) and

$(2N-5)$ angular variables ($\mathbf{Q}$) that are defined by $(N-2)$ polar angles $\{\theta_i\}$ and $(N-3)$ azimuthal angles $\{\varphi_j\}$ of the radial vectors in the body-fixed (BF) frame. The angular variables depend on the choice of the BF frame. By using the orthogonal polyspherical coordinates, the resulting Hamiltonian has many merits such as simplicity, a partitioned structure and the same formulation for general molecules.[8,31,32,40,85] By taking the advantage of the partitioned structure in orthogonal polyspherical coordinates, the Hamiltonian is written as[40,71]

$$\hat{H} = \hat{T}_R(\mathbf{R}) + \hat{H}_Q(\mathbf{Q};\mathbf{R}) \tag{1}$$

with

$$\hat{H}_Q(\mathbf{Q};\mathbf{R}) = \hat{T}_Q(\mathbf{Q};\mathbf{R}) + V(\mathbf{Q},\mathbf{R}), \tag{2}$$

where $V(\mathbf{Q},\mathbf{R})$ is the potential energy surface of the system. $\hat{T}_R(\mathbf{R})$ and $\hat{T}_Q(\mathbf{Q};\mathbf{R})$ are the kinetic energy operators in the radial and angular coordinates, respectively. The kinetic operator $\hat{T}_R$ is just a summation of one dimensional (1D) Hamiltonian $\hat{h}(r_i)$, i.e.,

$$\hat{T}_R(\mathbf{R}) = \sum_{i=1}^{N-1}[\hat{h}(r_i) - V_0(r_i)], \tag{3}$$

$$\hat{h}(r_i) = -\frac{\hbar^2}{2\mu_i r_i^2}\frac{\partial}{\partial r_i}r_i^2\frac{\partial}{\partial r_i} + V_0(r_i), \tag{4}$$

where $V_0(r_i)$ is a 1D reference potential in r_i with its associated reduced mass μ_i. And $\hat{T}_Q$ only parametrically depends on $\mathbf{R}$ through pre-factors without any crossed partial derivative terms between the two coordinate groups. Generally, it can be partitioned as

$$\hat{T}_Q(\mathbf{Q};\mathbf{R}) = \sum_{i=1}^{N-1}\frac{1}{2\mu_i r_i^2}\hat{T}_Q^{(i)}(\mathbf{Q}), \tag{5}$$

where $\hat{T}_Q^{(i)}(\mathbf{Q})$ are R-independent.

The eigenvalues of $\hat{H}$ is solved using the standard Lanczos method[42]

$$\beta_{j+1}|\psi_{j+1}> = \hat{H}|\psi_j> - \alpha_j|\psi_j> - \beta_j|\psi_{j-1}>, \tag{6}$$

where α_j and β_j are the mean energy and residual of the jth vector respectively. They are defined as

$$\alpha_j =< \psi_j|\hat{H}|\psi_j >,\ \beta_{j+1} =< \psi_{j+1}|\hat{H}|\psi_j > \tag{7}$$

with

$$\beta_1 = 0,\ |\psi_0 >= 0. \tag{8}$$

Therefore the Lanczos recursion reduces the original Hamiltonian matrix to a symmetric tridiagonal form

$$\mathbf{T}_K = \begin{bmatrix} \alpha_1 & \beta_2 & & & \\ \beta_2 & \alpha_2 & \beta_3 & 0 & \\ & \beta_3 & \ddots & \ddots & \\ & 0 & \ddots & \ddots & \beta_K \\ & & & \beta_K & \alpha_K \end{bmatrix}. \tag{9}$$

The three term recurrence starts with an initial random Lanczos vector $|\psi_1 >$. In matrix form Eq. (6) is expressed as

$$\hat{H}\mathbf{V}_K = \mathbf{V}_{K+1}\mathbf{T}_K = \mathbf{V}_K\mathbf{T}_K + \beta_{K+1}\psi_{K+1}e_K^T. \tag{10}$$

Here $'T'$ refers to transpose, and e_j is a unit vector in the jth dimension. $\mathbf{V}_K = \{|\psi_1 >, |\psi_2 >, \cdots, |\psi_K >\}$ is the Lanczos vector matrix with a size K.

Although the standard Lanczos method is very simple and powerful, it is difficult to use for the computation of the eigenvectors of large system. This is largely due to the loss of orthogonality of Lanczos vectors and the long iterations required for convergence. In this work, we instead use the guided spectral transform Lanczos (GSTL) algorithm[49,68] if both the eigenvalues and eigenvectors are wanted. Similar to the standard recursion, the GSTL method is written as

$$\beta_{j+1}|\psi_{j+1} >= F(\hat{H})|\psi_j > -\alpha_j|\psi_j > -\beta_j|\psi_{j-1} >, \tag{11}$$

or in the matrix form

$$F(\hat{H})\mathbf{V}_K = \mathbf{V}_{K+1}\mathbf{T}_K = \mathbf{V}_K\mathbf{T}_K + \beta_{K+1}\psi_{K+1}e_K^T, \tag{12}$$

where $F(\hat{H})$ is a guided spectral transform function of $\hat{H}$. It is expanded in a short series of formally orthogonal Lanczos (FOL) polynomials ($\mathcal{L}_k(\hat{H})$),[12,69,86] i.e.

$$F(\hat{H}) = \sum_{k=1}^{L_C} A_k(E_{ref})\mathcal{L}_k(\hat{H}). \tag{13}$$

The FOL polynomials are defined by the pre-calculated Lanczos parameters (α_k, β_k) as

$$\beta_{k+1}\mathcal{L}_{k+1} = \hat{H}\mathcal{L}_k - \alpha_k\mathcal{L}_k - \beta_k\mathcal{L}_{k-1}, \tag{14}$$

with

$$\mathcal{L}_0(\hat{H}) = 0 \text{ and } \mathcal{L}_1(\hat{H}) = 1.$$

By using the property of the Lanczos polynomials

$$< E'|\mathcal{L}(\hat{H})|E >= \mathcal{L}(E)\delta_{EE'}, \tag{15}$$

one can write the transformed spectral curve as

$$F(E) = \sum_{k=1}^{L_C} A_k(E_{ref})\mathcal{L}_k(E). \tag{16}$$

It also defines the relationship between the eigenvalues (denoted E_n and $F_n(E_n)$ respectively) of $\hat{H}$ and $F(\hat{H})$. On the other hand, both $\hat{H}$ and $F(\hat{H})$ share the same eigenvectors.

In Eq. (13) the expansion coefficients $\mathbf{A}_k^T = \{A_1(E_{ref}), A_2(E_{ref}), \cdots, A_k(E_{ref})\}$ are determined by the guidance of the Green operator

$$\hat{G}(E_{ref}) = \frac{1}{\hat{H} - E_{ref}} \tag{17}$$

with a given reference energy (E_{ref}). Then they are obtained by solving the linear minimal residual (MINRES) equation[48,87]

$$\mathbf{L}_k\mathbf{L}_k^T\mathbf{A}_k = ((\mathbf{T}_k - E_{ref}\mathbf{I})^2 + \beta_{k+1}^2 e_k e_k^T)\mathbf{A}_k = (\mathbf{T}_k - E_{ref}\mathbf{I})e_1. \tag{18}$$

The linear equation can be easily solved using a LQ factorization method.[17,87] The expansion order L_C is determined by the criterion $|A_{L_C}| < 0.01$ as recommended.[12,68,69] It

should be mentioned that the Green operator is used just as guidance for the spectral transform, and is never to be converged. In other words, the resulting spectral transform function may not look like a Kronecker delta-function here.

The GSTL algorithm has been widely used in quantum scattering and molecular spectroscopy calculations in the past decade. The reader can see the recent review[8] and references therein. In those applications, the $F(\hat{H})$ functions are commonly expanded in Chebyshev polynomials. In contrast, here, the FOL polynomials are employed. The use of FOLs is somewhat preferable. For instance, the expansion coefficients are optimal with respect to the system of interest as the Lanczos parameters used are produced using the system Hamiltonian. If one selects the reference energy E_{ref} close to the vibrational ground state of $\hat{H}$, it is more efficient to compute the lowest eigenstates.

In short, the GSTL method using the FOL polynomials involves two loops of Lanczos iterations. The outer loop is shown in Eq. (11). The inner loop is used to carry out the $F(\hat{H}) - |\psi_j >$ products using the pre-defined parameters $\{L_C, A_k, \alpha_k, \beta_k\}$.

2.2 Dipole transition strength

Within the dipole approximation, the infrared vibrational transition intensity from an initial state i to a final state f can be determined from the quantity[88,89]

$$D(\nu_{if}) = \sum_{\eta=x,y,z} |\mu_\eta^{if}|^2, \tag{19}$$

with

$$|\mu_\eta^{if}| = | < \psi_i|\mu_\eta|\psi_f > | = \left\{ \sum_{a,b} | < \psi_i^a|\mu_\eta|\psi_f^b > |^2 \right\}^{1/2}, \tag{20}$$

where a and b refer to the summation of degenerate states of the ith and f^{th} energy states (denoted $|\psi_i(E_i) >$ and $|\psi_f(E_f) >$ respectively) if any. $\nu_{if} = |E_f - E_i|$ is the transition energy, and μ_η are the Cartesian components of the dipole moment in the molecule-fixed frame.

For a large polyatomic molecule, the basis size representing wavefunctions of eigenstates is often huge. Thus it is formidable to get many state wavefunctions for evaluating the average values $|\mu_\eta^{if}|$ in Eq. (20) explicitly. In order to avoid this difficulty, we employ the elegant recursive residue generation method.[44,72–75] The RRGM approach uses the standard Lanczos iterations to calculate the spectral density for a given initial normalized vector $|\phi_0>$ via Green operator $\hat{G}(E)$, i.e.[73,76]

$$G_{00}(E) =< \phi_0|\hat{G}(E)|\phi_0 >=< \phi_0|\frac{1}{\hat{H}-E}|\phi_0 > . \tag{21}$$

By using the identity in a set of orthonormal basis set $\{|\psi_f^b(E_f)>\}$

$$\sum_f \sum_b |\psi_f^b(E_f)><\psi_f^b(E_f)| = I, \tag{22}$$

the spectral density is obtained as

$$G_{00}(E) = \sum_f \sum_b < \phi_0|\psi_f^b > \frac{1}{E_f - E} < \psi_f^b|\phi_0 >= \sum_f \frac{R_{00}(E_f)}{E_f - E}, \tag{23}$$

with the diagonal residue at the energy pole E_f

$$R_{00}(E_f) = \sum_b | < \phi_0|\psi_f^b > |^2 = | < \phi_0|\psi_f > |^2, \tag{24}$$

or

$$R_{00}(E_f) = \lim_{E\to E_f} (E_f - E)G_{00}(E). \tag{25}$$

In particular, if one carries out K (large enough) standard Lanczos iterations with an initial Lanczos vector $|\psi_1 >= |\phi_0 >$ in Eq. (6), the element $G_{00}(E)$ is then determined by[72,73]

$$G_{00}(E) = \frac{\det[\mathbf{T}_K - E\mathbf{I}]^r}{\det[\mathbf{T}_K - E\mathbf{I}]}, \tag{26}$$

where the superscript r refers to the reduced matrix obtained by removing the first row and column from $[\mathbf{T}_K - E\mathbf{I}]$. With the help of the eigenvalues (denoted $\{\lambda_k\}$ and $\{\lambda_k^r\}$ respectively) of the tridiagonal matrices $\mathbf{T}_K$ and $\mathbf{T}_K^r$, the ratio of determinants reads

$$G_{00}(E) = \frac{\Pi_{k=1}^{K-1}(\lambda_k^r - E)}{\Pi_{k=1}^{K}(\lambda_k - E)}. \tag{27}$$

Now, let $|\phi_0>$ be $\mu_\eta|\psi_i(E_i)>/w_{\eta i}$ with the normalization factor $w_{\eta i}$. By using Eqs. (24-25) and (27), the final dipole transition element becomes

$$|\mu_\eta^{if}| = w_{\eta i}\left\{\lim_{E\to E_f}\frac{(E_f-E)\Pi_{k=1}^{K-1}(\lambda_k^r-E)}{\Pi_{k=1}^{K}(\lambda_k-E)}\right\}^{1/2}. \tag{28}$$

Therefore, for a given initial state $|\psi_i(E_i)>$, the transition elements to all final states $|\psi_f>$ are calculated with a single Lanczos recursion. It is worthwhile to point out that the RRGM algorithm has correctly taken the energy degeneracy into account, and the loss of orthogonality of Lanczos vectors has a negligible effect on results.[72–74] The eigenvalues of tridiagonal matrix $\mathbf{T}_K$ can be easily solved using a LQ factorization method that has a nice CPU time scaling as $\mathcal{O}(K^2)$. Most importantly, no explicit wavefunction other than the initial state is required in the calculations.

2.3 Initial vibrational wavefunction

The initial vibrational state $|\psi_i(E_i)>$ used above is computed using the GSTL algorithm in Eq. (11) via a Green function $\hat{G}(E_{FD})$-guided functional $F(\hat{H})$. That is, the wavefunction is built up as

$$|\psi_i(E_i)>=\sum_{k=1}^{K}B_{ki}|v_k> \tag{29}$$

in the Lanczos subspace $\{|v_k>\}$, where B_{ki} is the eigenvector of state E_i. In this eigenstate calculation, one needs only to perform the $\hat{H}-|v_k>$ products. Following the same techniques used in our two-layer Lanczos iteration method, those products are carried out in a combined grid/diabatic basis functions in which the Lanczos vector $|v_k>$ is expressed as

$$|v_k>=\sum_{m,\alpha}C_{m,\alpha}^k f_m(\mathbf{Q};\mathbf{R}_0,\mathbf{R}_0^V)|\mathbf{R}_\alpha>, \tag{30}$$

where $|\mathbf{R}_\alpha>=\Pi_{i=1}^{N-1}|r_{\alpha_i}>$ refer to the direct-product PO-DVR functions in the radial coordinates; and α being a collective DVR index. The 1D PO-DVRs are calculated using the lowest eigenstates of the Hamiltonian $\hat{h}(r)$ in Eq. (4). In this work, the direct-product

basis functions are further contracted by discarding those PO-DVRs where the minimum potential energies in their corresponding $\mathbf{R}_\alpha$ sectors are larger than a threshold value (V_{th}).[12,40,41]

In Eq. (30) f_m are the vibrationally diabatic basis functions in the angular variables $\mathbf{Q}$ as they are independent of the $\mathbf{R}$ coordinates. They are formed by the lowest eigenstates of a reference reduced-dimension Hamiltonian $\hat{H}^0_Q(\mathbf{Q};\mathbf{R}_0,\mathbf{R}^V_0)$ in $\mathbf{Q}$, namely

$$\hat{H}^0_Q(\mathbf{Q};\mathbf{R}_0,\mathbf{R}^V_0)f_m(\mathbf{Q};\mathbf{R}_0,\mathbf{R}^V_0) = \mathcal{E}^0_m f_m(\mathbf{Q};\mathbf{R}_0,\mathbf{R}^V_0), \tag{31}$$

with

$$\hat{H}^0_Q(\mathbf{Q};\mathbf{R}_0,\mathbf{R}^V_0) = \hat{T}_Q(\mathbf{Q};\mathbf{R}_0) + V(\mathbf{Q};\mathbf{R}^V_0), \tag{32}$$

where $\mathbf{R}_0$ are the radial references in the kinetic energy operator. Usually, they are constant as $\{r_{i0}\}$. $\mathbf{R}^V_0$ are the references in the potential energy surface. In contrast, $\mathbf{R}^V_0$ can be selected as a function of $\mathbf{Q}$ in order to define a good reference potential. For instance, the reference potential is obtained by partially optimizing the radial variables for every given $\mathbf{Q}$ values.[90]

Again, the eigen-equation in Eq. (31) is solved by the GSTL algorithm in Eq. (11) via another Green function $\hat{G}(E_Q)$-guided functional $F(\hat{H}^0_Q)$. In this step, a non-direct product FBR basis set $\{|l>\}$ is often employed in order to properly deal with the singularities in polar angles.[7,40] In FBR, the action of $\hat{H}^0_Q(\mathbf{Q};\mathbf{R}_0,\mathbf{R}^V_0)$ on a Lanczos vector $|v'_k>= \sum_l C^k_l|l>$ is performed as

$$\hat{H}^0_Q|v'_k>= \sum_l \sum_{i=1}^{N-1} C^k_l \frac{1}{2\mu_i r^2_{i0}} \hat{T}^{(i)}_Q(\mathbf{Q})|l> + \sum_{l'}\sum_l\sum_\gamma \mathbf{U}^\dagger_{l'\gamma} V(\mathbf{Q}_\gamma;\mathbf{R}^V_0)\mathbf{U}_{\gamma l} C^k_l|l'>, \tag{33}$$

where $\mathbf{U}$ is the collocation matrix between the FBR and DVR ($\{|\gamma>\}$) basis sets, i.e.

$$|\gamma>= \sum_l \mathbf{U}_{\gamma l}|l> . \tag{34}$$

Here one should note that l and γ are the collective FBR and DVR indices with a dimension of $2N-5$, respectively. Although the detailed formulae of $\hat{T}^{(i)}_Q$ and $\mathbf{U}$ are dependent of

the definition of $\mathbf{Q}$, usually, the $\hat{T}_Q^{(i)} - |l>$ products are analytically computed on-the-fly in FBR. They are very simple and easy. In practice, the last potential term in Eq. (33) is often carried out using a pseudo-spectral transformation technique.[91–93] As a result, the overall matrix-vector multiplications are efficiently accomplished by using a series of small sequential matrix-vector products in one-by-one degree, which avoids the direct multi-dimensional matrix multiplications. Nevertheless, in this circumstance, the DVR basis size is larger than the FBR, i.e., $\mathbf{U}^\dagger\mathbf{U} = \mathbf{I}$ but $\mathbf{U}\mathbf{U}^\dagger \neq \mathbf{I}$. For more details, the reader can see Refs. [85], [6, 85], [7] and [12, 31] for tri-, tetra-, penta- and hexa-atomic molecules, respectively. Therefore, the final diabatic basis function is obtained as

$$f_m(\mathbf{Q};\mathbf{R}_0,\mathbf{R}_0^V) = \sum_l P_{lm}|l>= \sum_\gamma X_{\gamma m}|\gamma>,\ m = 1, 2, \cdots, M \tag{35}$$

$$X_{\gamma m} = \sum_l \mathbf{U}_{\gamma l} P_{lm}, \tag{36}$$

where P_{lm} and $X_{\gamma m}$ are the eigenvector coefficients of f_m in FBR and DVR respectively.

Eventually, the key action of $\hat{H}$ on vector $|v_k>$ in the GSTL recurrence is written as

$$\begin{aligned}\hat{H}|v_k> \ &= \ \sum_{n,\beta}\sum_{m,\alpha}\Big\{<\mathbf{R}_\beta|\hat{T}_R(\mathbf{R})|\mathbf{R}_\alpha>\delta_{nm} + \mathcal{E}_m^0\delta_{nm}\delta_{\beta\alpha} \\ &\quad + <f_n|\Delta\hat{H}_Q(\mathbf{R}_\alpha)|f_m>\delta_{\beta\alpha}\Big\} C_{m,\alpha}^k f_n(\mathbf{Q};\mathbf{R}_0,\mathbf{R}_0^V)|\mathbf{R}_\beta>,\end{aligned} \tag{37}$$

with

$$<\mathbf{R}_\beta|\hat{T}_R(\mathbf{R})|\mathbf{R}_\alpha> \ = \ \sum_{i=1}^{N-1}\Big\{<r_{\beta_i}|\hat{h}(r_i)|r_{\alpha_i}> - V_0(r_{\alpha i})\delta_{\beta_i\alpha_i}\Big\} \times \Pi_{j\neq i}^{N-1}\delta_{\beta_j\alpha_j}, \tag{38}$$

$$<f_n|\Delta\hat{H}_Q(\mathbf{R}_\alpha)|f_m> \ = \ \sum_{i=1}^{N-1}\Delta I_{\alpha i0}(r_{\alpha i})<f_n|\hat{T}_Q^{(i)}|f_m> + <f_n|\Delta V(\mathbf{Q};\mathbf{R}_\alpha)|f_m>, \tag{39}$$

and

$$\Delta V(\mathbf{Q};\mathbf{R}_\alpha) \ = \ V(\mathbf{Q};\mathbf{R}_\alpha) - V(\mathbf{Q};\mathbf{R}_0^V), \tag{40}$$

$$\Delta I_{i0}(r_i) \ = \ \frac{1}{2\mu_i r_i^2} - \frac{1}{2\mu_i r_{i0}^2}, \tag{41}$$

Here the pre-factors $\Delta I_{i0}(r_i)$ have a diagonal matrix representation in DVR. The $R-$independent $\hat{T}_Q^{(i)}$ matrices need only be calculated once for all $\mathbf{R}_\alpha$ sets.[40] In addition, $<f_n|\Delta V(\mathbf{Q};\mathbf{R}_\alpha)|f_m>$

are the potential residual matrix elements. They are computed using a DVR representation of the diabatic functions. In practice, the upper or lower matrices of $\Delta\hat{H}_Q(\mathbf{R}_\alpha)$ are first evaluated, and saved on disk before the GSTL Lanczos iterations start.

By using Eq. (30), the initial vibrational wavefunction becomes

$$|\psi_i(E_i)>=\sum_{\alpha,m} b^i_{\alpha m} f_m(\mathbf{Q};\mathbf{R}_0,\mathbf{R}_0^V)|\mathbf{R}_\alpha> \tag{42}$$

with the coefficients

$$b^i_{\alpha m}=\sum_k B_{ki}C^k_{m,\alpha}. \tag{43}$$

Here $b^i_{\alpha m}$ has a dimension of N among which one dimension refers to the diabatic basis functions. In the latter calculations, only $b^i_{\alpha m}$ and $X_{\gamma m}$ are required. $X_{\gamma m}$ are saved on disk to reduce core memory usage, once the calculation of the potential residual matrix elements is complete.

2.4 Dipole wavefunction and DVR contraction

In this subsection we present a few practical techniques how to cope with the dipole-initial state product wavefunction

$$|\psi_{i,\eta}>=\mu_\eta|\psi_i(E_i)>=\sum_{\alpha,n} a^{i,\eta}_{\alpha n} f_n(\mathbf{Q};\mathbf{R}_0,\mathbf{R}_0^V)|\mathbf{R}_\alpha> \tag{44}$$

for a high dimension problem. Although the calculations of transition strengths are performed in a reduced N dimension manner as shown in Eq. (37), one has to access the full $(3N-6)$ dimension spatial space for computing $|\psi_{i,\eta}>$. If it is directly calculated in full dimension, we will encounter with not only a memory problem but also a CPU (central processing unit) time issue. For instance, as discussed below for the application of CH_4, the primitive DVR basis size is as large as 396 billion that require about 3168 GB memory to save a single vector. It is also time-consuming to evaluate the dipole moment surfaces on such a large set of grids. Our previous studies[12,40] have already shown that computing

potential energy points is one of two CPU-time dominant steps in the eigenvalue calculations with the two-layer Lanczos method. Indeed, it is the most CPU time-consuming step in the six-atomic molecule $(H_2)_3$ case owing to the complexity of the potential energy surface.[12] Calculating the dipole moment surfaces has the same issues as the potential energy surface.

In order to overcome those difficulties, here, we use the DVR contraction and partial transformation procedures. Firstly, the diabatic basis functions are truncated in DVR. The truncation procedure is done just after finishing the calculations of the $< f_n|\hat{T}_Q^{(i)}|f_m >$ matrices in Eq. (39). In this approach, the FBR diabatic functions are first transformed into their DVR functions $X_{\gamma m}$. Then, the compact DVR basis is obtained by discarding those DVR points where the potential energy values are larger than V_{th}. The truncation procedure could introduce some errors. However, the errors are negligible because the resulting diabatic functions often conserve their norms very well in the compact DVR basis owing to the large potential threshold V_{th}. Previous studies[41,94,95] have shown that the errors introduced into eigenvalues are small in the order of about 0.02 cm^{-1}. In this work the contracted DVR basis set is denoted as $\tilde{X}_{\tilde{\gamma}m}$ where the collective index $\tilde{\gamma}$ stands for the compact DVRs. The compact DVR basis functions are also used to construct the potential residual matrix elements in Eq. (39).

Secondly, the dipole-wavefunction coefficients are evaluated using the following partial transformation manner, i.e.

$$\tilde{a}^i_{\tilde{\gamma}\alpha}(\mathbf{R}_\alpha) = \begin{cases} \sum_m \tilde{X}_{\tilde{\gamma}m} b^i_{\alpha m}, & \text{if } (\sum_m |b^i_{\alpha m}|^2)^{1/2} \geq \epsilon_b \\ 0, & \text{otherwise} \end{cases} \tag{45}$$

and

$$a^{i,\eta}_{\alpha n} = \sum_{\tilde{\gamma}} \tilde{X}_{\tilde{\gamma}n} \tilde{d}^{i,\eta}_{\tilde{\gamma}\alpha}(\mathbf{R}_\alpha), \eta = x, y, z, \tag{46}$$

with

$$\tilde{d}^{i,\eta}_{\tilde{\gamma}\alpha}(\mathbf{R}_\alpha) = \begin{cases} \mu_\eta(\mathbf{R}_\alpha, \tilde{\gamma}) \tilde{a}^i_{\tilde{\gamma}\alpha}(\mathbf{R}_\alpha), & \text{if } |\tilde{a}^i_{\tilde{\gamma}\alpha}| \geq \epsilon_a \\ 0, & \text{otherwise} \end{cases} \tag{47}$$

for a given set of $\mathbf{R}_\alpha$ in the radial coordinates. As one can see, this calculation routine is performed in reduced dimension (i.e. $2N-5$ in $\mathbf{Q}$) instead of full dimension. Therefore, the memory problem is solved in addition to the numerical efficiency. This merit results from the use of DVR representation in the radial coordinates.

Furthermore, the conditions in Eqs. (45) and (47) are used to pre-screen those grids with negligible amplitude of the wavefunction at which the dipole-wavefunction values are approximately taken as zero. Vain numerical operations are avoided, saving further CPU time. Of course, the two criteria ϵ_a and ϵ_b selected should be small enough so that the truncated wavefunction density is small enough, e.g., say about 10^{-4} to preserve the accuracy of the calculated dipole transition strengths. This treatment has no influence on the eigenvalues.

2.5 Computational procedure and discussions

The multi-layer Lanczos iteration algorithm is depicted in Fig. 1. It involves two short standard Lanczos iterations, two GSTL propagations, and three times N_{init} (the number of initial vibrational states of interest) long standard Lanczos recurrences. The first short Lanczos iteration is to prepare the Lanczos coefficients for constructing the guided spectral transform function of $F(\hat{H}_Q^0)$ in the reduced dimension angular coordinates $\mathbf{Q}$ while the second short iteration is for the function $F(\hat{H})$ with the whole system Hamiltonian. In addition, the first GSTL propagation is used to calculate the vibrationally diabatic basis functions $\{f_m\}$ in terms of $F(\hat{H}_Q^0)$, and the second GSTL propagation is employed to obtain a few of the lowest vibrational wavefunctions of the system of interest by using $F(\hat{H})$. Those iterations and propagations start with a random vector. The last $3N_{init}$ long Lanczos recurrences are used to calculate the dipole transition strengths from a given initial vibrational state for each dipole moment component (x, y, z). That is, in this loop, the recurrences begin with an initial Lanczos vector defined by the dipole-wavefunction in Eq. (44). Importantly, those sequentially layered iterations are performed separately

so that they are able to share the same core memory. Thus the effort to calculate the dipole transition intensities is in the same order as pure eigenvalue calculations. Like the two-layer Lanczos method[40,71] all calculations are done in a reduced dimension manner without any dynamics approximation. Therefore this multi-layer Lanczos algorithm is a rigorous full dimension quantum dynamics method.

In particular, the algorithm is general and problem-independent for polyatomic molecules. This important feature is inherited from the same partitioned structure of quantum Hamiltonian in any set of orthogonal polyspherical coordinates. In addition, the large amplitude motions of vibrations are naturally described in terms of the use of scattering coordinates. By using the DVR representation, the resulting Hamiltonian matrices (e.g. see Eq. (37) are very sparse. Therefore the Hamiltonian matrix-vector products are always calculated on-the-fly without explicitly constructing any large Hamiltonian matrices. In other words, such a structure is very suitable for iterative diagonalizations and massive parallel computations.

In the multi-layer Lanczos algorithm, the time-limiting steps are the computations of the potential residual matrix elements $< f_n|\Delta V(\mathbf{Q};\mathbf{R}_\alpha)|f_m >$ and the diabatic basis functions as shown in Eq. (33). Fortunately, both the properties need only be calculated once. The diabatic function calculation is also the core memory-limiting step. Although the $\hat{H}_Q^0$ Hamiltonian is in reduced dimension, it still has $2N-5$ degrees of freedom. Therefore, the multi-layer Lanczos algorithm is applicable for polyatomic molecules with up to six atoms only. In the next section we will present an application to the benchmark five-atom molecule CH_4.

3 Application

The multi-layer Lanczos algorithm described above is universal, and requires only that the molecular Hamiltonian has the partitioned structure in Eqs. (1)-(5). Such a partitioned

Hamiltonian is always true in any set of orthogonal polyspherical coordinates regardless of the number of atoms in molecule.[6,7,31,85] Therefore, one can choose an optimal set of orthogonal polyspherical coordinates for the specific molecule of interest. In this section, we will present an application to calculating the energies and dipole intensities of methane CH_4 using the (4+1) Radau coordinates (see Fig. 2),[96,97] i.e., the "Icd=2" set in the PetroVib program.[7] The rovibrational spectrum of methane and isotopomers have extensively been studied during the last half century.[35,36,41,89,90,98–108] In this work, we mainly address the numerical demonstration of the algorithm for calculating the IR spectrum of CH_4. One should not expect spectroscopically accurate results owing to the limited accuracy of both potential energy and dipole moment surfaces.

3.1 Kinetic operator $\hat{T}_Q^{(i)}$ and numerical aspects

According to the definition of the coordinates for CH_4, we have four radial coordinates $\mathbf{R} = \{r_1, r_2, r_3, r_4\}$ and five angular variables $\mathbf{Q} = \{\theta_1, \varphi_1, \theta_2, \varphi_2, \theta_3\}$. The R-dependent kinetic operator $\hat{T}_R$ has been given in Eqs. (3) and (4). And the Q-dependent kinetic operator parts are given by[7]

$$\hat{T}_Q^{(i)}(\mathbf{Q}) = \hat{j}_i^2, \text{ i=1,2,3} \tag{48}$$

$$\hat{T}_Q^{(4)}(\mathbf{Q}) = \sum_{i=1}^{3} \hat{j}_i^2 + \sum_{i<k=1}^{3} (2\hat{j}_{iz}\hat{j}_{kz} + \hat{j}_{i+}\hat{j}_{k-} + \hat{j}_{i-}\hat{j}_{k+}), \tag{49}$$

where $\hat{j}_i$, $\hat{j}_{iz}$ and $\hat{j}_{i\pm}$ are the angular momentum, its Z projection and the ladder operators respectively.[109]

As usual, we use a symmetrically adapted FBR (SA-FBR) $|l>=|j_1j_2j_3nmp>$ in the angular coordinates. It is written as[7]

$$|l>= \frac{1}{\sqrt{2(1+\delta_{0n}\delta_{0m})}} \{|j_1j_2j_3nm> +(-1)^p|j_1j_2j_3-n-m>\} \tag{50}$$

where p refers to the parity of inversion symmetry. $|jm>$ are the orthonormal spherical

harmonic basis functions,[109] i.e.,

$$< \theta, \varphi | jm >= \Theta_j^m(\theta) \frac{1}{\sqrt{2\pi}} e^{im\varphi}, \tag{51}$$

where $\Theta_j^m(\theta)$ are the normalized associated Legendre polynomials. These functions are the common eigenstates of both $\hat{j}^2$ and $\hat{j}_z$, namely,

$$\hat{j}^2 | jm > \;=\; j(j+1)\hbar^2 | jm >, \tag{52}$$

$$\hat{j}_z | jm > \;=\; m\hbar | jm > . \tag{53}$$

For the ladder operators, we have the relationship,

$$\hat{j}_\pm | jm >= [j(j+1) - m(m \pm 1)]^{1/2} \hbar | jm \pm 1 > . \tag{54}$$

Therefore the T_Q-FBR basis products can be easily computed by using Eqs. (52)-(54). The detailed expressions are given in Ref. [7]. Furthermore, the corresponding collocation matrix in Eq. (33) is then written as

$$\mathbf{U} = CST_{2D} \mathbf{\Theta}_{\theta_3}^{(n+m)} \mathbf{\Theta}_{\theta_2}^{(m)} \mathbf{\Theta}_{\theta_1}^{(n)} \tag{55}$$

where CST_{2D} is the two-dimensional cosine/sine transformation in the two azimuthal angles (φ_1, φ_2) while the $\Theta_\theta^{(k)}$ are the one-dimensional collocation matrices in θ. They are defined by the normalized associated Legendre polynomials in Eq. (51).[6,7,110] As a result, the matrix multiplications are performed by a series of sequential low dimensional matrix multiplications using the $\mathbf{U}$ matrix in Eq. (55).

The total Hamiltonian is represented in a combined FBR/DVR basis set. Ten potential optimized DVR (PO-DVR) points are used for each radial coordinate. The non-direct product FBR in the angular variables are formed by the largest quantum number $j_{max} = 28$. The symmetrically adapted DVR basis with respect to inversion symmetry is used with respect to the SA-FBR. The potential threshold value is set at $V_{th} = 2.75\,\mathrm{eV}$ for the DVR basis contraction. The primitive DVR basis sizes are 3.96×10^7 (or a basis set of

5.65×10^6 FBR functions) in $\mathbf{Q}$ that leads to a basis set of 3.96×10^{11} in total. 440 diabatic basis functions and 19 lowest state wavefunctions are calculated. The criteria used for DVR contraction are $\epsilon_a = 10^{-6}$ and $\epsilon_b = 2 \times 10^{-4}$ (see Eqs. (45) and (47)) in the dipole transition strength calculations.

The T8 potential energy surface of Schwenke and Partridge[103] (labeled as SP(T8) in the literature) is employed to compute the vibrational energy levels and wavefunctions of CH_4. The SP(T8) surface is an accurate global *ab initio* potential energy surface for vibrational states up to 5000 cm^{-1}.[41,90,111] The dipole transition strengths are computed using the first order expansion of the *ab initio* dipole moment surfaces (DMS) of Yurchenko et al.[89] Using the truncated DMS is to avoid the unphysical interpolations at large geometry distortions[89] although they are one of the best dipole surfaces near the equilibrium geometry of CH_4. In the calculations, the reference radial coordinates in the kinetic energy operators are 2.05791 a_0 for r_{i0} with its associated mass $\mu_i = 1.0072764$ amu. As in previous works,[41,90,103,105] we have employed nuclear masses of atoms, *i.e.*, 1.0072764 amu for H and 11.9967085 amu for C in order to be consistent with the convention of the SP(T8) potential.

3.2 Results and discussion

The parameters used in the guided spectral transform functions are listed in Table 1 where the Lanczos coefficients are obtained using the $\hat{H}_Q^0$ (or $\hat{H}$) Hamiltonian with a random initial Lanczos vector. The expansion coefficients are computed with a reference of $E_{ref} = 0.45$ eV for $F(\hat{H}_Q^0)$ or $E_{ref} = 1.25$ eV for $F(\hat{H})$. The reference energies are selected to be close to the zero-point energy levels of the corresponding Hamiltonians in order to calculate the lowest eigenstates. Figure 3 shows the guided spectral profiles. As expected, the spectra have strongly been dilated at low energies so that the low-lying eigenstates can be converged quickly. Furthermore, the curves resemble an exponential function although a Green operator is used as guidance. This is due to the low order expansion of the formally

orthogonal Lanczos polynomials.[69] Actually it is the desired spectral transform shape. A δ-function is unwanted here for the calculations of many states.

Our calculations have converged the vibrational energies up to 6200 cm^{-1} within 0.05 cm^{-1}. The obtained energies are in excellent agreement with previous best theoretical results[90,111] based on the same SP(T8) surface.[103] The total dipole transition spectrum up to 6200 cm^{-1} from the vibrational ground state is shown in Fig. 4. Since this work focuses on the study of transition strengths, a trivial comparison of energies will not be given here except for the F_2-symmetry levels having strong dipole transition intensities. They are listed in Table 2, where the energy levels are labeled as "$(v_1v_3)(v_2v_4)$symmetry" following the polyad notation of Wang and Carrington.[41,111] $v_1(A_1)$ and $v_3(F_2)$ are the stretch modes of CH_4 while $v_2(E)$ and $v_4(F_2)$ are the bend ones.

Overall, the computed values are in good agreement with the theoretical[89] and experimental[99–101,112–115] results. The vibrational band intensities from the energy level E_i are calculated by[2,89,112,113]

$$S = \frac{8\pi^3 10^{-36}}{3hcQ_v(T)} \frac{LT_0}{T} e^{-E_i/k_BT} \nu_{if} (1 - e^{-hc\nu_{if}/k_BT}) |\mu^{if}|^2, \tag{56}$$

where $L = 2.686754 \times 10^{19}$ cm^{-3} is the Loschmidt's number. $T_0 = 273.15$ K is the reference temperature. Q_v is the vibrational partition function of CH_4. As expected, the SP(T8) surface[103] has about 10 cm^{-1} errors in energy. Since Yurchenko et al.[89] used a refined potential energy surface, more accurate frequencies are obtained. In particular, our calculated band intensities are consistent with those of Yurchenko and co-workers although this work used only the first order truncated DMS of them. This is not surprising because the first order expansion is a good approximation for the vibrational ground state. Nevertheless, a better agreement should not be expected. Importantly, such a numerical demonstration really verifies that this algorithm works well.

Secondly, the accuracy of the algorithm has been tested. For instance, by using the explicit wavefunctions, the dipole transition elements in Debye for the $(00)(00)A_1 \rightarrow (00)(01)F_2$

transition at 1312 cm^{-1} are obtained as

$$[|\mu_X^{if}|, |\mu_Y^{if}|, |\mu_Z^{if}|]^b = \begin{bmatrix} -0.053036 & 0.014073 & 0.011647 \\ -0.030079 & 0.016723 & 0.021064 \\ -0.015815 & 0.009807 & 0.058884 \end{bmatrix} \tag{57}$$

or

$$[|\mu_X^{if}|, |\mu_Y^{if}|, |\mu_Z^{if}|] = [0.062990, 0.023956, 0.063614], \tag{58}$$

which are accurately reproduced. This results from the merit that the RRGM method is capable of describing the degenerate states correctly. On the other hand, if one uses the arithmetic average method, the results obtained are

$$[|\mu_X^{if}|, |\mu_Y^{if}|, |\mu_Z^{if}|] = [0.035514, 0.013319, 0.039535] \tag{59}$$

which are smaller than the accurate values. Therefore, one should be careful to use the transition amplitudes involving degenerate states by using the arithmetic average method. As the individual transition strength $\mu_\alpha^{if,b} =< \psi_i|\mu_\alpha|\psi_f^b >$ is not necessary to be same for those degenerate levels, in general, we have

$$\sum_b (N_C^b |\mu_\alpha^{if,b}|^2) / \sum_b N_C^b \neq \sum_b |\mu_\alpha^{if,b}|^2, \tag{60}$$

where N_C^b are the copy number of the converged states. Obviously, Eq. (60) holds only if N_C^b are the same for all degenerate states $|\psi_f^b >$. In addition, those individual transition components also depend on the orientation of the body-fixed frame although their total value is independent of it.

Finally, as we expected, the "GSTL iteration with $F(\hat{H}_Q^0)$" step (see Fig. 1) dominates the allocation of CPU time. On a CRAY XC30 machine with 12 CPUs, this step took about 186 hours (without the factor of 12 for the sake of simplicity) in which 41 hours were used for computing the 440 diabatic functions and 145 hours for the construction of potential residual matrices. It cost only 0.95 hours in the "GSTL iteration with $F(\hat{H})$" step for computing the 19 eigenstate wavefunctions. In the "Do dipole moment loop" step, the allocation of CPU time were 17.4 hours (3×5.8) for 9000 Lanczos iterations of each dipole

component, where near half hour was spent to obtain the dipole-wavefunction products. The CPU time in all other steps is negligible. Therefore, the CPU time ratio of the IR spectrum to pure vibrational state calculations is roughly 1.065 ((186+0.95+17.4)/(186+5.8)). In other words, compared to the study of pure vibrational energies, the cost increases about 6.5% for the IR calculations. No additional core memory is required to compute the IR spectrum beyond that needed for vibrational energies in the "GSTL iteration with $F(\hat{H}_Q^0)$" step.

4 Conclusion

We have developed a multi-layer Lanczos algorithm for computing vibrational energies and dipole transition intensities of polyatomic molecules with the help of the elegant recursive residue generation method (RRGM), the guided spectral transform Lanczos technique, the reduced dimension strategy of the two-layer Lanczos method, and DVR basis contraction. The two latter techniques allow us to construct (dipole-) eigenstate wavefunctions without explicitly accessing the huge primitive basis set, which makes it possible to calculate the vibrational spectra of large molecules. The algorithm uses only an initial state wavefunction in a reduced dimension basis set to give its transition spectrum to all final states with a single Lanczos propagation. No product wavefunction is needed. Furthermore, it is a rigorous full dimensional quantum dynamics algorithm without any dynamics approximation. In particular, the algorithm is general and problem-independent for polyatomic molecules. The large amplitude motions of vibrations are naturally described in terms of the use of scattering coordinates, i.e., the orthogonal polyspherical coordinates.

An application is presented by calculating the infrared vibrational dipole transition spectrum of CH_4 based on the *ab initio* T8 potential energy surface of Schwenke and Partridge and the low-order truncated *ab initio* dipole moment surfaces of Yurchenko and co-workers. Results shows that the multi-layer Lanczos method is very promising. Now the

multi-layer Lanczos algorithm has been implemented with the PetroVib program.[7] Therefore, it becomes a routine to calculate both the vibrational energies and dipole transition intensities of a general five-atomic molecule in a rigorous full dimension approach once a global potential energy surface and dipole moment surfaces are provided.

This algorithm is also applicable for studying vibrational Raman polarizability active spectra as they can be determined from the quantities[116]

$$|a^{if}_{\eta\eta'}| = | < \psi_i|a_{\eta\eta'}|\psi_f > |, \tag{61}$$

where $a_{\eta\eta'}$ $(\eta, \eta' = x, y, z)$ are the polarizability tensor matrices. One can see that Eq. (61) is in the same form as Eq. (20). Therefore, the vibrational Raman spectra can be done in the same manner once the dipole surfaces are replaced with the polarizability tensors. But we have to run six times for each independent tensor component instead of three in the dipole case for a given initial state.

Essentially, the algorithm requires only the action of the two Hamiltonians ($\hat{H}^0_Q$ and $\hat{H}$) on Lanczos vectors. This is very similar to those powerful time-dependent or real wavepacket methods[8,10,16,37,77,78] for calculating transition amplitudes. Recently, Hammer and Manthe[16] have used a Lanczos-tpye iteration approach using a energy-filtered operator for calculating dipole transition strengths of polyatomics with up to nine atoms in MCTDH. Their calculations also started with a dipole-ground state wavefunction as an initial Lanczos vector. In this work, the key condition is that the resulting Hamiltonian matrices are sparse regardless of the choice of coordinates. Otherwise, the efficiency of the algorithm will reduce owing to the expensive cost for performing Hamiltonian-vector products with a dense matrix, which likes all other iterative methods. For a semi-rigid molecule, a set of non-orthogonal coordinates are often optimal for studying the low-lying vibrational states.[1] If a proper set of basis functions are used, the Hamiltonian matrix can still be sparse in non-orthogonal coordinates but with more samll low rank (often rank 2 due to the crossed terms in kinetic energy operators between two coordinate variables) matrix

blocks. In this circumstance, the cost of calculations of Hamiltonian-vector products could be compensated by shorter Lanczos iterations for convergence. Indeed, more future work is needed to explore this topics.

Acknowledgments

This work was performed at Brookhaven National Laboratory under Contract No. DE-AC02-98CH10886 with the U.S. Department of Energy and supported by its Division of Chemical Sciences, Office of Basic Energy Sciences. It also used the resource at the National Energy Research Scientific Computing Center (NERSC) under Contract No. DE-AC02-05CH11231. The author thanks Professor Sergey Yurchenko for providing the FORTRAN code of dipole moment surfaces.

References

[1] A.G. Csazar, C. Fabri, T. Szidarovsky, E. Matyus, T. Furtenbacher, and G. Czako, *Phys. Chem. Chem. Phys.* **14**, 1085 (2012).

[2] S. Carter, A.R. Sharma, J.M. Bowman, P. Rosmus, and R. Tarroni, *J. Chem. Phys.* **131**, 224106 (2009).

[3] N.C. Handy, S. Carter, and S.M. Colwell, *Mol. Phys.* **96**, 477 (1999).

[4] I.N. Kozin, M.M. Law, and J. Tennyson et al., *Comp. Phys. Comm.* **163**, 117 (2004).

[5] C. Leforestier, F. Gatti, R.S. Fellers, and R.J. Saykally, *J. Chem. Phys.* **117**, 8710 (2002).

[6] H.-G. Yu and J.T. Muckerman, *J. Mol. Spectrosc.* **214**, 11 (2002).

[7] H.-G. Yu, *J. Mol. Spectrosc.* **256**, 287 (2009).

[8] G. Nyman and H.-G. Yu, *Int. Rev. Phys. Chem.* **32**, 39 (2013).

[9] A. Valdes, R. Prosmiti, and G. Delgado-Barrio, *J. Chem. Phys.* **136**, 104302 (2012).

[10] H.-D. Meyer, F. Gatti, and G. A. Worth eds, *Multidimensional Quantum Dynamics: MCTDH Theory and Applications* (Wiley-VCH, Weinheim, Germany, 2009).

[11] F. Huarte-Larrañaga and U. Manthe, *J. Chem. Phys.* **117**, 4635 (2002).

[12] H.-G. Yu, *J. Chem. Phys.* **120**, 2270 (2004).

[13] X.G. Wang and T. Carrington Jr., *J. Chem. Phys.* **129**, 234102 (2008).

[14] O. Vendrell, F. Gatti, and H.-D. Meyer, *J. Chem. Phys.* **127**, 184303 (2007).

[15] M. Schroder, F. Gatti, and H.-D. Meyer, *J. Chem. Phys.* **134**, 234307 (2011).

[16] T. Hammer and U. Manthe, *J. Chem. Phys.* **136**, 054105 (2012).

[17] G.H. Golub and C.F. VanLoan, *Matrix Computations, 3rd* (The Johns Hopkins University Press, Baltimore, 1996).

[18] Y. Saad, *Numerical Methods for Large Eigenvalue Problems* (Manchester Unversity Press, Manchester, UK, 1992).

[19] H. Guo, *Rev. Comput. Chem.* **25**, 285 (2007).

[20] W. Chen and B. Poirier, *J. Theor. Comput. Chem.* **9**, 825 (2010).

[21] J.C. Light, I.P. Hamilton, and J.V. Lill, *J. Chem. Phys.* **82**, 1400 (1985).

[22] J.C. Light and T. Carrington Jr., *Adv. Chem. Phys.* **114**, 263 (2000).

[23] B. Poirier and J.C. Light, *J. Chem. Phys.* **111**, 4869 (1999).

[24] V. Szalay, *J. Phys. Chem. A* **117**, 7075 (2013).

[25] J. Echave and D.C. Clary, *Chem. Phys. Lett.* **190**, 225 (1992).

[26] H. Wei and T. Carrington, Jr., *J. Chem. Phys.* **97**, 3029 (1992).

[27] D.J. Haxton, *J. Phys. B* **40**, 4443 (2007).

[28] U. Manthe, *J. Chem. Phys.* **130**, 054109 (2009).

[29] H.-G. Yu, *J. Chem. Phys.* **122**, 164107 (2005).

[30] A. Leclerc and T. Carrington Jr., *J. Chem. Phys.* **140**, 174111 (2014).

[31] F. Gatti and C. Iung, *Phys. Rep.* **484**, 1 (2009).

[32] C. Iung and F. Gatti, *Int. J. Quantum Chem.* **106**, 130 (2006).

[33] V. Szalay, *J. Chem. Phys.* **140**, 234107 (2014).

[34] H. Koppel, L.S. Cederbaum, and W. Domcke, *J. Chem. Phys.* **77**, 2014 (1982).

[35] C. Iung and C. Leforestier, *J. Chem. Phys.* **102**, 8453 (1995).

[36] C. Iung, C. Leforestier, and R.E. Wyatt, *J. Chem. Phys.* **98**, 6722 (1993).

[37] V.A. Mandelshtam and H.S. Taylor, *J. Chem. Phys.* **106**, 5085 (1997).

[38] V.A. Mandelshtam and H.S. Taylor, *Phys. Rev. Lett.* **78**, 3278 (1997).

[39] P. Pendergast, Z. Darakjian, E.F. Hayes, and D.C. Sorensen, *J. Compt. Phys.* **113**, 201 (1994).

[40] H.-G. Yu, *J. Chem. Phys.* **117**, 8190 (2002).

[41] X.-G. Wang and T. Carrington Jr., *J. Chem. Phys.* **121**, 2937 (2004).

[42] C. Lanczos, *J. Res. Nat. Bur. Stand.* **45**, 255 (1950).

[43] T. Ericsson and A. Ruhe, *Math. Comput.* **35**, 1251 (1980).

[44] R.E. Wyatt, *Phys. Rev.* **E51**, 3643 (1995).

[45] F. Webster, P.J. Rossky, and R.A. Friesner, *Comp. Phys. Comm.* **63**, 494 (1991).

[46] H. Kono, *Chem. Phys. Lett.* **214**, 137 (1993).

[47] C. Leforestier, K. Yamashita, and N. Moiseyev, *J. Chem. Phys.* **103**, 8468 (1995).

[48] H.-G. Yu and S.C. Smith, *Ber. Bunsenges. Phys. Chem.* **101**, 400 (1997).

[49] H.-G. Yu and G. Nyman, *J. Chem. Phys.* **110**, 11133 (1999).

[50] S. Dallwig, N. Fahrer, and C. Schlier, *Chem. Phys. Lett.* **191**, 69 (1992).

[51] C. Iung and C. Leforestier, *J. Chem. Phys.* **97**, 2481 (1992).

[52] H.-G. Yu and G. Nyman, *Chem. Phys. Lett.* **298**, 27 (1998).

[53] B. Poirier and T. Carrington Jr., *J. Chem. Phys.* **114**, 9254 (2001).

[54] D. Neuhauser, *in Highly Excited Molecules: Relaxation, Reaction and Structure* (A.S. Mullin and G.S. Schatz eds., Chapt.2, pp.26, Americal Chemical Society, Washington D.C., 1997).

[55] D. Neuhauser, *J. Chem. Phys.* **93**, 2611 (1990).

[56] M.R. Wall and D. Neuhauser, *J. Chem. Phys.* **102**, 8011 (1995).

[57] V.A. Mandelshtam and H.S. Taylor, *J. Chem. Phys.* **102**, 7390 (1995).

[58] R. Chen and H. Guo, *J. Chem. Phys.* **105**, 1311 (1996).

[59] R. Chen and H. Guo, *J. Compt. Phys.* **136**, 494 (1997).

[60] R. Chen and H. Guo, *J. Chem. Phys.* **111**, 464 (1999).

[61] H.-G. Yu and S.C. Smith, *J. Chem. Soc., Faraday Trans. 2* **93**, 861 (1997).

[62] K. Wu, A. Canning, H.D. Simon, and L.-W. Wang, *J. Compt. Phys.* **154**, 156 (1999).

[63] D.C. Sorensen and C. Yang, *SIAM J. Matrix Anal. Appl.* **19**, 1045 (1998).

[64] B. Poirier and J. Carrington Jr., *J. Chem. Phys.* **116**, 1215 (2002).

[65] S.-W. Huang and T. Carrington, Jr., *J. Chem. Phys.* **114**, 6485 (2001).

[66] Y. Zhou, J.R. Chelikowsky, and Y. Saad, *J. Compt. Phys.* **274**, 770 (2014).

[67] T. Ikegami, T. Sakurai, and U. Nagashima, *J. Comput. App. Math.* **233**, 1927 (2010).

[68] H.-G. Yu and G. Nyman, *J. Chem. Phys.* **110**, 7233 (1999).

[69] H.-G. Yu, *J. Chem. Phys.* **141**, 244114 (2014).

[70] G. Nyman and H.-G. Yu, *Rep. Prog. Phys.* **63**, 1001 (2000).

[71] H.-G. Yu, *Chem. Phys. Lett.* **365**, 189 (2002); *Erratum* **367**, 791 (2003).

[72] A. Nauts and R.E. Wyatt, *Phys. Rev. Lett.* **51**, 2238 (1983).

[73] R.E. Wyatt, *Adv. Chem. Phys.* **73**, 231 (1989).

[74] A. Nauts, *Chem. Phys. Lett.* **119**, 529 (1985).

[75] A. Nauts and X. Chapuisat, *Phys. Rev. A* **32**, 3403 (1985).

[76] H.-G. Yu and S.C. Smith, *Chem. Phys. Lett.* **283**, 69 (1998).

[77] R.Q. Chen and H. Guo, *J. Chem. Phys.* **111**, 9944 (1999).

[78] R.Q. Chen and H. Guo, *J. Chem. Phys.* **114**, 1467 (2001).

[79] O. Kolin, C. Leforestier, and N. Moiseyev, *J. Chem. Phys.* **89**, 6836 (1988).

[80] C. Leforestier, A. Viel, F. Gatti, C. Muñoz, and C. Iung, *J. Chem. Phys.* **114**, 2099 (2001).

[81] F. Gatti, *Theoretica Chimica Acta* **116**, 60 (2006).

[82] Z. Bačić, *Comp. Phys. Comm.* **128**, 46 (2000).

[83] T.J. Lukka, *J. Chem. Phys.* **102**, 3945 (1995).

[84] M. Mladenović, *J. Chem. Phys.* **112**, 1070 (2000).

[85] M.J. Bramley and T. Carrington Jr., *J. Chem. Phys.* **99**, 8519 (1993).

[86] M.H. Gutknecht, *SIAM J. Matrix Anal. Appl.* **13**, 594 (1992).

[87] C.C. Paige and M.A. Saunders, *SIAM J. Numer. Anal.* **12**, 617 (1975).

[88] G. Herzberg, *Molecular Spectra and Molecular Structure II. Infrared and Raman Spectra of Polyatomic Molecules* (Krieger Publishing Company, Malabar, Florida, 1991).

[89] S.N. Yurchenko, J. Tennyson, R.J. Barber, and W. Thiel, *J. Mol. Spectrosc.* **291**, 69 (2013).

[90] H.-G. Yu, *J. Chem. Phys.* **121**, 6334 (2004).

[91] R.A. Friesner, *J. Chem. Phys.* **85**, 1462 (1986).

[92] C. Leforestier, *J. Chem. Phys.* **101**, 7357 (1994).

[93] H.-G. Yu, *Chem. Phys. Lett.* **281**, 312 (1997).

[94] R.A. Friesner, J.A. Bentley, M. Menou, and C. Leforestier, *J. Chem. Phys.* **99**, 324 (1993).

[95] H.-G. Yu, *J. Chem. Phys.* **125**, 204306 (2006).

[96] R. Radau, *Ann. Sci. Ecole Normale Supérior* **5**, 311 (1868).

[97] F.T. Smith, *Phys. Rev. Lett.* **45**, 1157 (1980).

[98] E.H. Richardson, S. Brodersen, L. Krause, and H.L. Welsh, *J. Mol. Spectrosc.* **8**, 406 (1962).

[99] R. Georges, M. Herman, J.-C. Hilico, and O. Robert, *J. Mol. Spectrosc.* **187**, 13 (1998).

[100] J.-C. Hilico, O. Robert, M. Loete, S. Toumi, A.S. Pine, and L.R. Brown, *J. Mol. Spectrosc.* **208**, 1 (2001).

[101] E. Venuti, L. Halonen, and R.G. Della Valle, *J. Chem. Phys.* **110**, 7339 (1999).

[102] T.J. Lee, J.M.L. Martin, and P.R. Taylor, *J. Chem. Phys.* **102**, 254 (1995).

[103] D.W. Schwenke and H. Partridge, *Spectrochimica Acta* **A57**, 887 (2001).

[104] D.W. Schwenke, *Spectrochimica Acta* **A58**, 849 (2002).

[105] J. Xie and J. Tennyson, *Mol. Phys.* **100**, 1623 (2002).

[106] S. Carter, H.M. Shnider, and J. M. Bowman, *J. Phys. Chem.* **A104**, 2355 (2000).

[107] H.-G. Yu, *J. Chem. Phys.* **117**, 2030 (2002).

[108] J.Y. Wu, X.C. Huang, and S. Carter et al., *Chem. Phys. Lett.* **426**, 285 (2006).

[109] A.R. Edmonds, *Angular Momentum in Quantum Mechanics* (Princeton University Press,, Princeton, NJ, 1960).

[110] G.C. Corey, J.W. Tromp, and D. Lemoine, *in NATO ARW Proceedings on Grid Methods in Atomic and Molecular Quantum Calculation* (Kluwer Academic, Dordrecht, The Netherland, 1993).

[111] X.-G. Wang and T. Carrington Jr., *J. Chem. Phys.* **119**, 101 (2003).

[112] L.R. Brown, M. Loete, and J. Hilico, *J. Mol. Spectrosc.* **133**, 273 (1989).

[113] J.C. Hilico, M. Loete, and L.R. Brown, *J. Mol. Spectrosc.* **152**, 229 (1992).

[114] O. Ouardi, J.C. Hilico, M. Loete, and L.R. Brown, *J. Mol. Spectrosc.* **180**, 311 (1996).

[115] S. Albert, S. Bauerecker, V. Boudon, L.R. Brown, J.P. Champion, M. Loete, A. Nikitin, and M. Quack, *Chem. Phys.* **356**, 131 (2009).

[116] V. Barone, M. Biczysko, and J. Bloino, *Phys. Chem. Chem. Phys.* **16**, 1759 (2014).

Table 1: Parameters used in the guided spectral transform functions $F(\hat{H}_Q^0)$ and $F(\hat{H})$. All units are in eV.

Function	k	α_k	β_k	A_k
$F(\hat{H}_Q^0)$	1	8.21513982	0.0	0.14617555
	2	9.85952164	2.72459589	-0.04963823
	3	10.61340640	3.46931589	0.01997182
	4	10.83134600	3.87337344	-0.00824994
	5	10.91429670	4.08729944	0.00268117
	6	–	4.24630998	
$F(\hat{H})$	1	7.19160774	0.0	0.18935762
	2	7.21051576	1.77365660	-0.07074326
	3	7.14451184	2.38605981	0.03650476
	4	7.00083633	2.63358606	-0.01872734
	5	7.16833841	2.57112439	0.00660002
	6	–	2.45822701	

Table 2: A comparison of vibrational frequencies ν_{if} in cm^{-1}, dipole transition strengths $|\mu^{if}|$ in D and band intensities S in $cm^{-1}atm^{-2}$ at $T = 278.15\,K$ for the transition from the vibrational ground state to the F_2 vibrational states of CH_4.

	This work[a]			WC[111,a]	Y[90,a]	YTBT[89]		Expt.[99–101,115]	
label	ν_{if}	$\lvert\mu^{if}\rvert_{cal}$	S_{cal}	ν_{if}	ν_{if}	ν_{if}	$\lvert\mu^{if}\rvert_{cal}$	ν_{if}	S_{obs}
(00)(01)F_2	1312.18	0.09267	115.043	1311.74	1311.75	1310.87	0.09831	1310.76	127.68
(00)(02)F_2	2617.10	0.02111	11.920	2616.24	2616.24	2614.32	0.00706	2614.26	1.05
(00)(11)F_2	2831.56	0.02230	14.392	2831.53	2831.53	2830.28	0.01797	2830.32	6.63[b]
(01)(00)F_2	3014.57	0.08199	207.109	3013.60	3013.43	3019.49	0.09370	3019.49	269.92
(00)(03)F_2	3875.94	0.00609	1.469	3874.75	3874.73	3870.49	0.00401	3870.49	0.59[b]
(00)(03)F_2	3936.61	0.00275	0.303	3935.34	3935.34	3930.81	0.00288	3930.92	0.14[b]
(00)(12)F_2	4145.28	0.00166	0.116	4144.88	4144.85	4142.99	0.00295	4142.86	0.34
(10)(01)F_2	4222.76	0.00378	0.616	4221.85	4221.72	4223.52	0.01343	4223.46	7.84
(01)(01)F_2	4315.64	0.01050	4.865	4314.23	4314.06	4319.43	0.01593	4319.21	10.24
(00)(21)F_2	4349.71	0.00153	0.104	4350.10	4350.07	4348.97	0.00252	4348.71	0.55[b]
(00)(21)F_2	4379.31	0.00212	0.202	4379.77	4379.75	4379.15	0.00023	4378.98	0.23[b]
(01)(10)F_2	4538.30	0.00938	4.077	4537.82	4537.67	4543.90	0.00678	4543.76	1.26
(00)(04)F_2	5150.71	0.00160	0.135	5150.56	5149.13	5143.25	0.00060	5143.24	0.01
(00)(04)F_2	5217.30	0.00073	0.028	5216.98	5215.66	5210.65	0.00037	5211.29	
(00)(13)F_2	5376.36	0.00067	0.025	5383.09	5375.58	5370.37	0.00023	5376.95	
(00)(13)F_2	5435.09	0.00070	0.027	5440.67	5434.34	5429.07	0.00101	5429.58	
(00)(13)F_2	5449.35	0.00070	0.027	5455.06	5448.69	5444.87	0.00020	5445.12	
(10)(02)F_2	5522.28	0.00232	0.306	5521.21	5520.84	5519.47	0.00019	5517.17	
(01)(02)F_2	5586.85	0.00125	0.089	5585.36	5584.80	5586.76	0.00270	5587.98	
(01)(02)F_2	5613.59	0.00169	0.163	5612.27	5611.63	5620.63	0.00129	5623.01	
(01)(02)F_2	5624.86	0.00072	0.030	5625.32	5623.11	5633.69	0.00176	5628.40	
(00)(22)F_2	5645.32	0.00075	0.032	5651.12	5645.28	5643.64	0.00009	5640.66	
(00)(22)F_2	5670.76	0.00098	0.055	5676.63	5670.76	5668.70	0.00047	5668.98	
(10)(11)F_2	5725.66	0.00287	0.481	5725.66	5725.13	5727.16	0.00028	5729.68	
(01)(11)F_2	5818.02	0.00680	2.750	5817.23	5816.63	5823.03	0.00368	5826.65	
(01)(11)F_2	5839.90	0.00233	0.324	5839.47	5838.92	5843.72	0.00089	5849.30	
(11)(00)F_2	5855.94	0.01075	6.916	5853.96	5853.28	5861.92	0.00054	5819.72	
(00)(31)F_2	5867.54	0.00238	0.339	5872.47	5868.38	5868.23	0.00046	5867.66	
(00)(31)F_2	5895.14	0.00078	0.036	5900.48	5895.19	5894.54	0.00013	5894.12	
(02)(00)F_2	5992.71	0.00466	1.333	5993.51	5992.44	6004.45	0.00522	6004.69	1.63
(01)(20)F_2	6048.18	0.00212	0.278	6048.22	6047.96	6054.67	0.00094	6054.64	
(01)(20)F_2	6059.64	0.00172	0.184	6060.06	6059.67	6065.26	0.00095	6065.32	

[a] Results calculated on the SP(T8) potential energy surface; [b] The total intensity of this band.

Figure 1: A schematic flow chart of the multi-layer Lanczos iteration algorithm for computing vibrational energies and dipole transition strengths

Figure 2: The (4+1) Radau coordinates for CH_4, where the body-fixed Z-axis is coincident with the Radau vector $\mathbf{r}_4$ while the vector $\mathbf{r}_3$ lies in the XZ-plane toward the positive X direction.

Figure 3: Spectral transform curves $F(\hat{H}_Q^0)$ and $F(\hat{H})$ for the calculations of the diabatic basis functions and the lowest vibrational wavefunctions respectively.

Figure 4: Calculated dipole transition strengths from the vibrational ground state of CH_4.

Multi-layer Lanczos Iteration Algorithm

A short (50) simple Lanczos iteration with $\hat{H}_Q^0(Q)$
determine a spectral function $F(\hat{H}_Q^0)$

GSTL iteration with $F(\hat{H}_Q^0)$ for computing $\{f_m\}$
Outer-layer loop
recursion with $F(\hat{H}_Q^0)$
Inner-layer loop
recursion with $\hat{H}_Q^0(Q)$

A short (50) simple Lanczos iteration with $\hat{H}$
determine a spectral function $F(\hat{H})$

GSTL iteration with $F(\hat{H})$ for computing $\{|\psi_i>\}$
Outer-layer loop
recursion with $F(\hat{H})$
Inner-layer loop
recursion with $\hat{H}$

Do dipole moment loop
Obtain the dipole-wavefunction $|\psi_{i,\eta}>$
A long Lanczos iteration of $\hat{H}$ with $|\psi_{i,\eta}>$
Calculate eigenvalues and transition strengths

Fig. 1

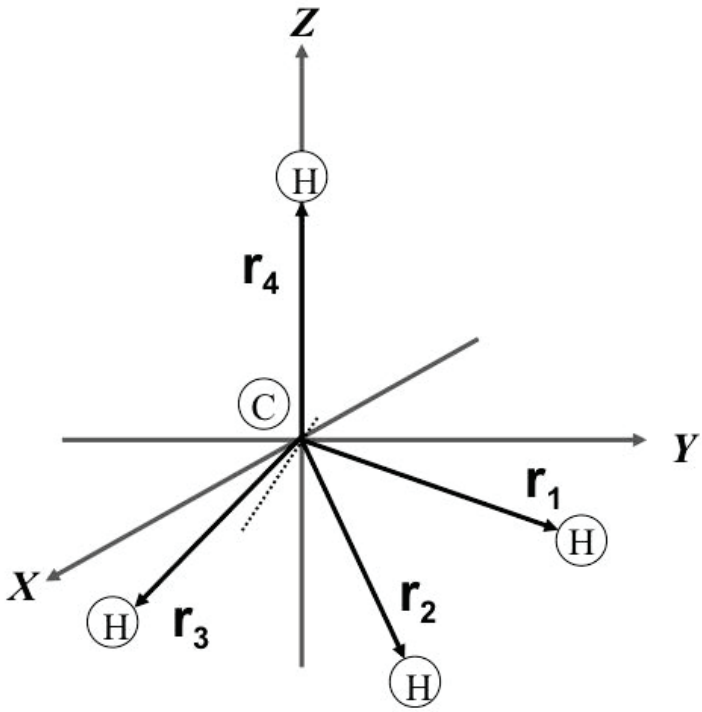

Fig. 2

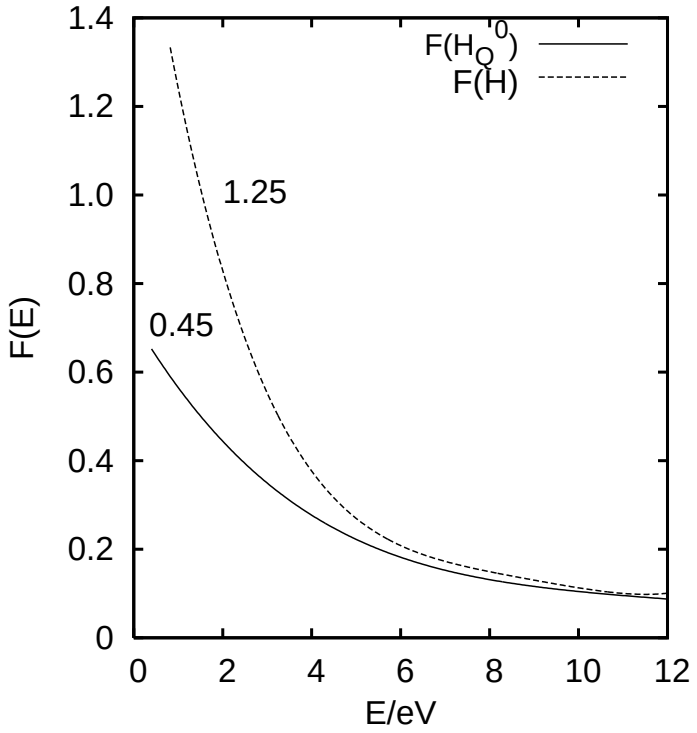

Fig. 3

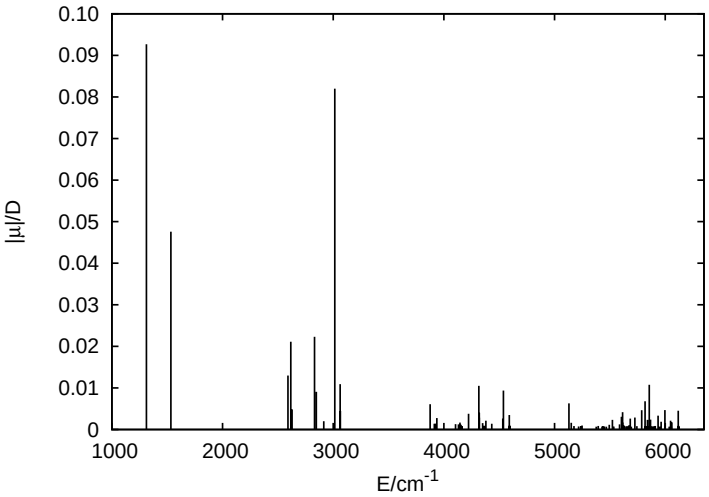
0.10
0.09
0.08
0.07
0.06
0.05
0.04
0.03
0.02
0.01
0
|μ|/D
1000
2000
3000
4000
5000
6000
E/cm-1

Fig. 4